Ancient TL

Athermal stability, bleaching behavior and dose response of luminescence signals from almandine and kyanite

Ian del Río[1*], André Oliveira Sawakuchi[2], Daniele Giordano[3], Thays Desiree Mineli[2], Luciana Nogueira[2], Tsegaye Abede[4], Daniel Atencio[2]

[1] Departamento de Ciencias Geológicas, Universidad Católica del Norte, Avenida Angamos 0610, Antofagasta, Chile
[2] Department of Sedimentary and Environmental Geology, Institute of Geosciences, University of São Paulo, Rua do Lago 562, São Paulo, SP, 05508-080, Brazil
[3] Earth Sciences Department, University of Torino, Via Valperga Caluso 35, 10125, Torino, Italy
[4] Adana Geological Consulting Company, Via Martin Luther King 9, 56021, Cascina, Italy

*Corresponding Author: iandelriogarcia@gmail.com

Received: April 4, 2019; in final form: June 18, 2019

Abstract

In order to evaluate the suitability of minerals other than quartz and feldspar for luminescence dating of sediments, luminescence properties from almandine and kyanite relevant for dosimetry such as luminescence signal stability, bleachability by sunlight exposure, and dose response are investigated. Thermoluminescence (TL) signals (UV emission) from almandine aliquots present athermal instability for the entire tested TL temperature range (25 – 450 °C). Almandine also presents a significant infrared stimulated luminescence (IRSL), post-infrared IRSL (post-IR IRSL) and optically stimulated luminescence (OSL) (blue stimulation and UV detection) signals. Kyanite aliquots show a TL glow curve (UV emission) characterized by four distinct peaks at temperatures of around 90, 170, 220 and 325 °C. The 325 °C TL peak seems to be stable, without significant decay after 6.8 hours of storage at room temperature (25 °C). Kyanite aliquots did not yield significant IRSL or post-IR IRSL signals, but OSL is observed in the UV detection window. Fading tests for the OSL signals resulted in g-values of 15.8 ± 2.8 %/decade for almandine and 21.2 ± 11.6 %/decade for kyanite. The OSL signals are bleachable by sunlight with 34% to 50% of signal remaining after 5 minutes of light exposure. Both minerals yielded dose recovery ratios close to unity (given dose of 100 Gy) and the dose response curves had a high D_0 values of around 800 Gy.

Keywords: Thermoluminescence; IRSL; OSL; Almandine; Kyanite; Luminescence dating

1. Introduction

Although quartz and feldspar are the major components of terrigenous sediments, the heavy mineral suite (density >2.85 g/cm^3) includes several minerals whose luminescence properties have been poorly investigated for dating purposes. In this context, silicates from the garnet group such as almandine ($Fe_3Al_2(SiO_4)_3$, ~ 4.31 g/cm^3) and aluminosilicates such as kyanite ($Al_2(SiO_4)O$, ~ 3.67 g/cm^3) are typical minerals in the heavy mineral assemblage of sands worldwide (Morton & Hallsworth, 1994, 1999). Both minerals occur in metamorphic rocks that experienced medium to high pressure and temperature conditions (100 – 2000 MPa and 200 – 1000 °C) equivalent to greenschist and eclogite facies (Deer et al., 2013). These rocks are common sources of sediments in cratonic geological settings like Brazil (Almeida et al., 2000). Almandine and kyanite show high resistance to physical and chemical weathering in comparison to other com-

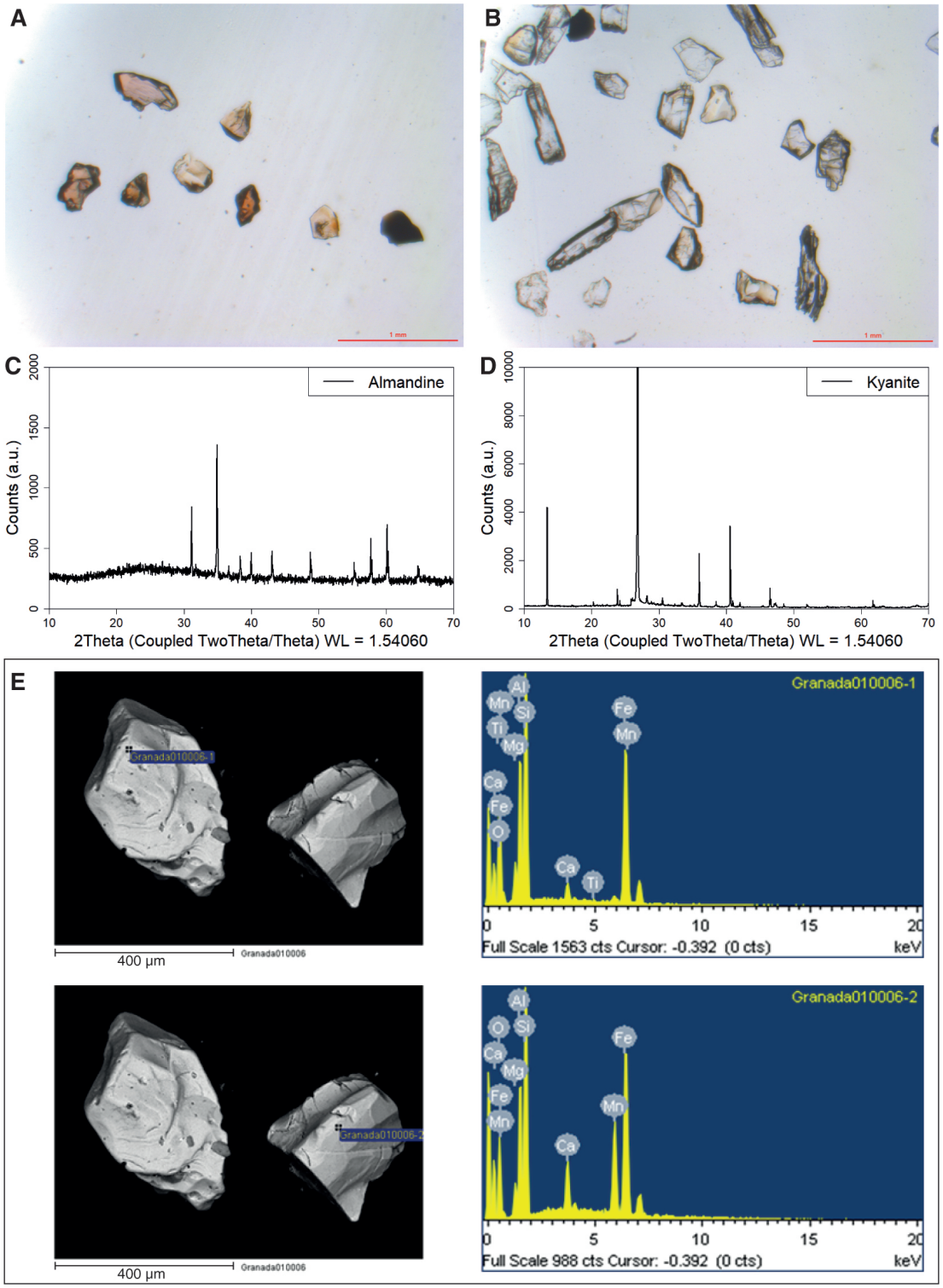

Figure 1. Almadine (A) and kyanite (B) grains under the optical microscope. XRD spectra of studied almandine (C) and kyanite (D) samples. E) Scanning electron microscope image (secondary electrons detector, left) from grains of almandine and energy dispersive spectrum (right) showing the chemical composition corresponding to the points highlighted in the images at left.

mon heavy minerals such as pyroxene and amphibole (Morton & Hallsworth, 1999). This property allows their transport over long distances and preservation in sediments. Detrital grains of almandine and kyanite typically account for between 5 and 20% of the heavy mineral suite of sands (Morton & Hallsworth, 1999; Rimington et al., 2000; Guedes et al., 2011; do Nascimento Jr et al., 2015).

Among the few studies on luminescence signals of heavy

Step	Procedure
1	Dose D_x
2	Preheat at 200°C for 10s
3	Blue stimulation at 125°C for 40s (L_x)
4	Test dose Dt
5	Preheat at 160°C for 0s
6	Blue stimulation at 125°C for 40s (T_x)
7	Blue stimulation at 280°C for 40s
8	Return to 1

Table 1. Measurement protocol (Murray & Wintle, 2003) applied to build dose response curves and estimate equivalent doses using the OSL signal from almandine and kyanite.

minerals, Watanabe et al. (2015) demonstrated that heavy minerals such as beryl and pyroxene show thermoluminescence (TL) signals with dose response curves reaching high saturation doses (>1000 Gy) compared to quartz optically stimulated luminescence (OSL) and feldspar infrared stimulated luminescence (IRSL) or post-infrared IRSL (post-IR IRSL) signals. However, the TL signals measured by Watanabe et al. (2015) as well as other previous studies that focused on TL signals of heavy minerals such as synthetic diopside-like crystals (Cano et al., 2008), kyanite (Souza et al., 2003) and andalusite (Cano et al., 2011) did not evaluate the dose response curves of luminescence signals corrected for sensitivity changes, and no information was provided for OSL or post-IR IRSL signals successfully used for luminescence dating.

This contribution investigates TL, OSL, IRSL and post-IR IRSL signals from almandine and kyanite. Particularly for the OSL signal, this includes the evaluation of bleaching performance, fading rates and dose response curves from both minerals.

2. Materials and methods

The studied almandine and kyanite crystals were obtained from the mineral collection of the Istituto di Geoscienze e Georisorse (Pisa, Italy). All samples were mechanically crushed and wet sieved to isolate the 180 – 250 µm grain-size interval. The purity of almandine and kyanite concentrates were assessed by means of optical microscopy (Fig. 1A, 1B) and X-ray diffraction (XRD) analysis (Fig. 1C, 1D). Scanning electron microscopy with energy dispersive spectroscopy (SEM/EDS) showed that the studied almandine grains contain relatively low amounts of magnesium. Since iron was the most abundant cation found in the studied samples (Fig. 1E), in the following section, we will refer to the mineral species as almandine for clarity.

Luminescence measurements were performed using a Risø TL/OSL DA-20 reader equipped with a $^{90}Sr/^{90}Y$ beta source, delivering a dose rate of 0.111 ± 0.003 Gy/s for discs and 0.099 ± 0.003 Gy/s for cups. We highlight that these beta source dose rates were determined using a quartz (2.65 g/cm^3) calibration standard (Hansen et al., 2015) which has lower density than almandine (~ 4.31 g/cm^3) and kyanite (~ 3.67 g/cm^3). Nathan et al. (2003) found a difference of ~ 30% for the beta dose rates in steel (7.9 g/cm^3) and glass (2.65 g/cm^3) spheres. Thus, the doses given in this study for almandine and kyanite aliquots are apparent doses. The mentioned doses are not accurate and must be considered only for evaluation of luminescence properties.

Optical stimulation used arrays of blue LEDs (470 ± 20 nm) at 90% power density (~ 40 mW/cm^2) and IR LEDs (870 ± 20 nm) also at 90% power density (~ 130 mW/cm^2). Light emissions were recorded through a Thorn EMI 9235QB photomultiplier. The OSL signal was measured with blue stimulation and light detection in the UV spectral range (290-370 nm) using a Hoya U-340 detection filter. The IRSL and post-IR IRSL signals were measured in the blue-violet window (340-480 nm) using a Corning 7-59 and Schott BG-39 filter combination. The TL emission was recorded both in the UV and blue-violet windows. Grains of almandine or kyanite were mounted on stainless steel discs (9.7 mm diameter) and cups (11.7 mm diameter) using silicone spray. Each aliquot contained ~ 500 grains covering the entire disc or cup to maximize signal intensity. Also, large aliquots minimize potential effects induced by variation in composition (i.e. cation concentration) of almandine grains from different aliquots.

After irradiating the almandine and kyanite aliquots with doses of 50, 100, 500 and 1000 Gy, TL glow curves were obtained in the UV and blue-violet detection windows. TL measurements were performed from room temperature (~ 25 °C) to 450 °C using a heating rate of 5 °C/s. In order to assess the stability of TL peaks and detect athermal loss of signal, or fading, aliquots from almandine and kyanite were irradiated with 200 Gy and TL signals were measured after storage at room temperature (~ 25 °C) for increasing times (0 to 6.82 hours) following an approach, similar to the fading measurements for IRSL signals (Auclair et al., 2003). Additionally, the response of TL signals to light exposure was evaluated for both minerals. For this experiment, a 200 Gy dose was administered to two aliquots of each mineral, which were exposed to a solar simulator lamp for 0, 2.5 and 5 hours.

The presence of IRSL (at 50 °C) and post-IR IRSL signals was checked for aliquots of almandine and kyanite. Aliquots were irradiated with 50 Gy and preheated at 250 °C (60 s) or 320 °C (60 s) for measurement of post-IR IRSL signals at 225 °C for 100 s (Buylaert et al., 2009) or at 290 °C for 200 s (Buylaert et al., 2012), respectively.

The OSL decay curves (100 s of blue light stimulation at 125 °C) were recorded for aliquots irradiated with 100 Gy and preheated for 10 s at temperatures of 25, 160, 200, 220, 260 and 300 °C. Linear modulated optically stimulated luminescence (LM-OSL) curves were obtained by linearly increasing the blue LED power intensity from 0 to 90% for 5000 s after giving a 200 Gy dose and a 200 °C preheat (10 s). The preheat temperature applied in LM-OSL measurements was defined after evaluation of the OSL signal depletion for preheat temperatures from 25 to 300 °C. A preheat temperature of 200 °C was used based on the intensity of initial

emission of the OSL decay curve of both minerals. This preheat temperature apparently eliminates less stable components, but still preserves a detectable emission in the initial 1 s of the OSL decay curve, which is analogous to the fast OSL component of quartz (Jain et al., 2003). The OSL signal measured with a preheat treatment at 200 °C for 10 s and corrected for a test dose signal (Table 1) was used in experiments to evaluate fading rate, bleachability and dose response.

The OSL signal was calculated from the first second of the OSL decay curve and the last 10 seconds were used as background. Fading rates for the OSL signal were estimated following Auclair et al. (2003). For this, three aliquots of each mineral type were irradiated with a 300 Gy dose, preheated to 200 °C and stimulated with blue LEDs after storage times between 0.4 and 55 hours. Sensitivity variation between measurements was corrected by a test dose of 100 Gy. In this study, g-values were calculated following Huntley & Lamothe (2001) and normalized to a measurement delay time of 2 days after irradiation.

The bleachability of the OSL signal was examined by administering a dose of 50 Gy to aliquots exposed to a solar simulator lamp from 5 minutes to 5 hours. Before each measurement, the aliquots were preheated to 200 °C. The dose response of the OSL signal was evaluated using a single-aliquot regenerative (SAR) dose protocol (Murray & Wintle, 2003) as described in Table 1. The dose response curves were built by administrating increasing doses (D_1<D_2<D_3<D_4) up to 2500 Gy and a test dose (D_t) of 100 Gy to control sensitivity changes during consecutive measurements. A 0 Gy dose (D_5) was given to estimate recuperation and a repetition of the first cycle (D_6 = D_1) to calculate the recycling ratio. A single saturating exponential growth function was used for fitting the dose response curves and calculation of characteristic dose (D_0). To assess the ability of OSL from the studied almandine and kyanite aliquots to recover a known dose under laboratory conditions, a dose recovery test was performed for a given dose of 100 Gy and using the protocol described in Table 1. Grain samples were exposed to light for long time (> 1 year) during their storage as museum specimens. The aliquots were further stimulated with blue light for 200 s at 280 °C prior to dose recovery tests, ensuring the

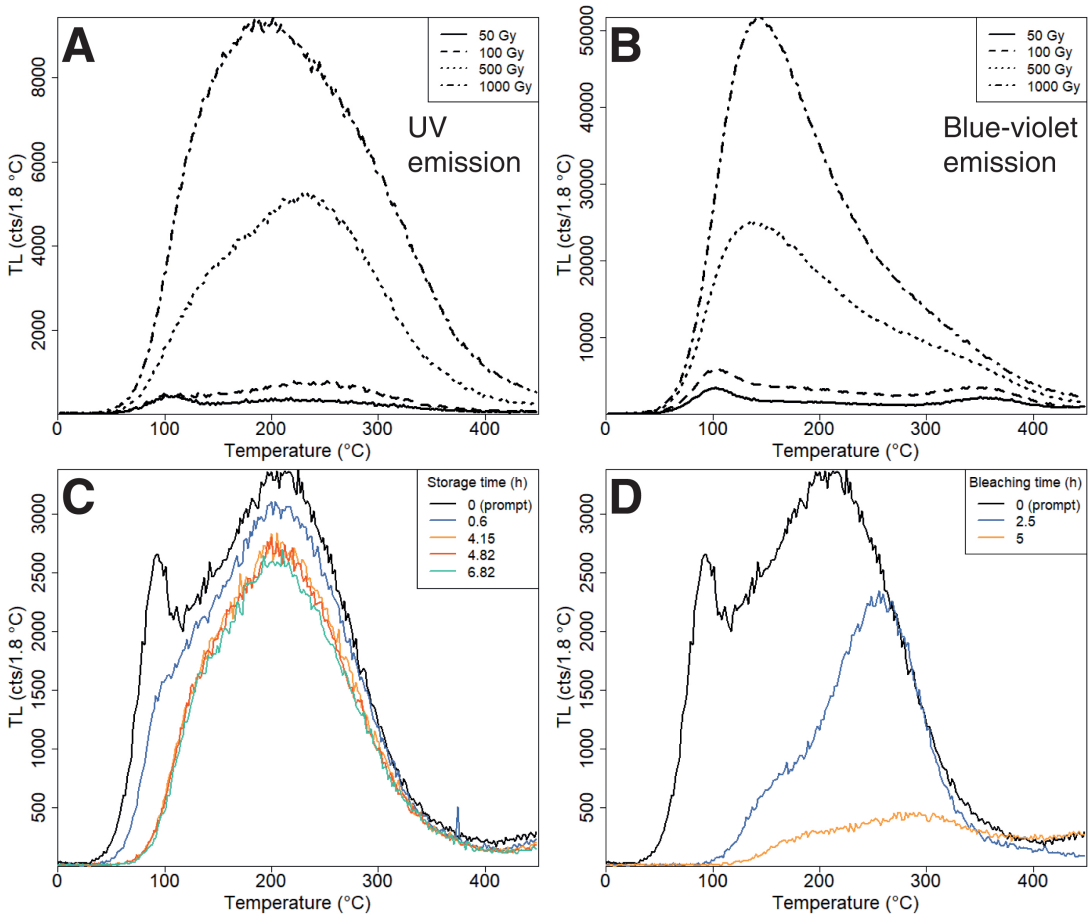

Figure 2. TL glow curves for the UV (A) and blue-violet (B) emissions of almandine. C) TL glow curves recorded after different storage times at room temperature (given dose of 200 Gy). D) TL glow curves recorded after different bleaching times under a solar simulator lamp. Note that the same TL measurement (0 storage or bleaching time) is used as reference for both stability and bleaching tests. Successive measurements were performed on the same aliquots.

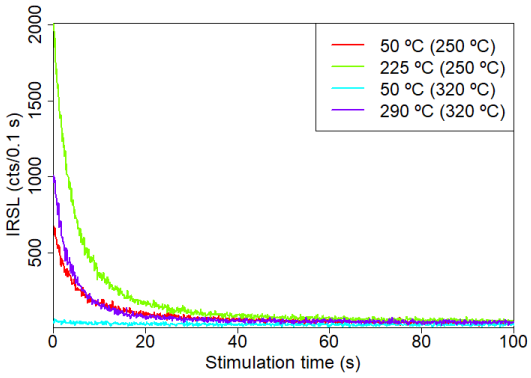

Figure 3. IRSL (at 50°C) and post-IR IRSL (at 225 and 290 °C) signals from almandine. For the IRSL and post-IR IRSL signals measured after a preheat of 320 °C, only the first 100 s of light emission are shown. The preheat temperatures are shown in brackets.

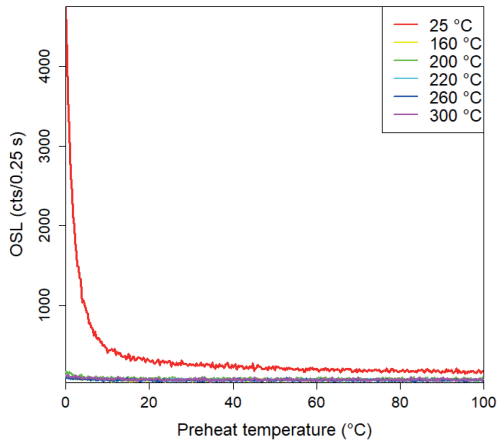

Figure 4. OSL decay curves of almandine measured for different preheat temperatures (from 25 to 300 °C). Aliquots were irradiated with 100 Gy.

bleaching of signals from natural residual doses. The data analysis were performed using the software *Analyst* (v4.52; Duller 2015) and the **R** package `'Luminescence'` (Kreutzer et al., 2012).

3. Results

3.1. Almandine

For the UV detection window, almandine TL curves (Fig. 2A) exhibit a peak at 100 °C, more noticeable at lower doses (50 Gy), followed by a broad peak from 150 to 350 °C, centered at about 220 °C. For doses higher than 100 Gy, a broad TL peak appears centered in the 200 – 240 °C interval, merging with the 100 °C peak and hindering the identification of other peaks. In the blue-violet detection window, TL peaks at 100 and 360 °C are recognized at doses up to 100 Gy. At higher doses, the 360 °C peak is hidden below the broad tail of the 100 °C peak (Fig. 2B). The TL (UV emission) of almandine aliquots decays significantly after 0.5 hours of storage under room temperature, but this is more notable for the 100°C TL peak (Fig. 2C). Regarding the bleachability of TL in the UV emission, the 100 °C TL peak was totally depleted after 2.5 hours of light exposure (Fig. 2D). However, the high instability of this peak at room temperature hinders the evaluation of its bleaching rate. After 5 hours of light exposure, there is significant depletion of the TL curve (25 – 450 °C) with a low intensity peak at 300 °C. Higher temperature TL peaks (> 200 °C) are highly depleted when aliquots are exposed to light, pointing to a significant bleaching (Fig. 2D).

Almandine shows significant IRSL and post-IR IRSL signals (Fig. 3). IRSL signals measured at 50 °C have a lower intensity than post-IR IRSL signals measured at 225 or 290 °C.

The OSL intensity from almandine decreases with the increase of preheat temperature (Fig. 4). OSL decay curves measured after a preheat with temperature from 160 to 300 °C display intensities (initial 1 s) almost 40 times lower than OSL curve obtained without preheat ("room temperature preheat" of 25 °C) (Fig. 4). The LM-OSL curve shows a well-defined peak in the first 100 s of light stimulation (Fig. 5A). Deconvolution into discrete components suggests the presence of four OSL components with photoionisation cross-section values of $1.21 \pm 0.13 \times 10^{-17}$, $1.68 \pm 0.18 \times 10^{-18}$, $8.87 \pm 2.8 \times 10^{-20}$ and $6.23 \pm 1.1 \times 10^{-22}$ cm^2.

Fading tests confirm the presence of athermal loss of the studied OSL signal from almandine that can be well-described as a logarithmic decay. The estimated average g-value is 15.8 ± 2.8 %/decade (Fig. 5B). The OSL signal decreases with light exposure (Fig. 5C). After 5 minutes of light exposure, remaining OSL signals amount to 34% of the initial signal (50 Gy). After 5 hours of light exposure, the OSL signal remaining is 8% of the initial signal. The dose response curve (Fig. 5D) of the OSL signal is well described by a single-saturating exponential function, showing relatively high saturation levels, with an average D_0 value of 791 Gy (n=2). Dose recovery tests resulted in an average calculated-to-given ratio of 0.98 ± 0.04 (for a given dose of 100 Gy), with aliquots yielding recuperation less than 0.1% and an average recycling ratio of 1.07 ± 0.04 (Table 2).

3.2. Kyanite

In the UV emission, kyanite TL curves reveal peaks at 90, 170, 220 and 325 °C (Fig. 6A). The TL peaks at 170, 220 and 325 °C grow up to a dose of 1000 Gy while the 90 °C TL peak reaches saturation at lower doses. TL curves of the blue-violet emission resemble the TL in the UV emission, with peaks at 90, 170 and 220 and a lower intensity peak at 325 °C (Fig. 6B). TL peaks (UV emission) of kyanite show differential decay when aliquots are stored under room temperature, with peaks at 90 and 170 °C presenting faster decay (Fig. 6C). However, the 325 °C TL peak is relatively stable for storage times up to 6.82 hours. Intensities of the 90, 170

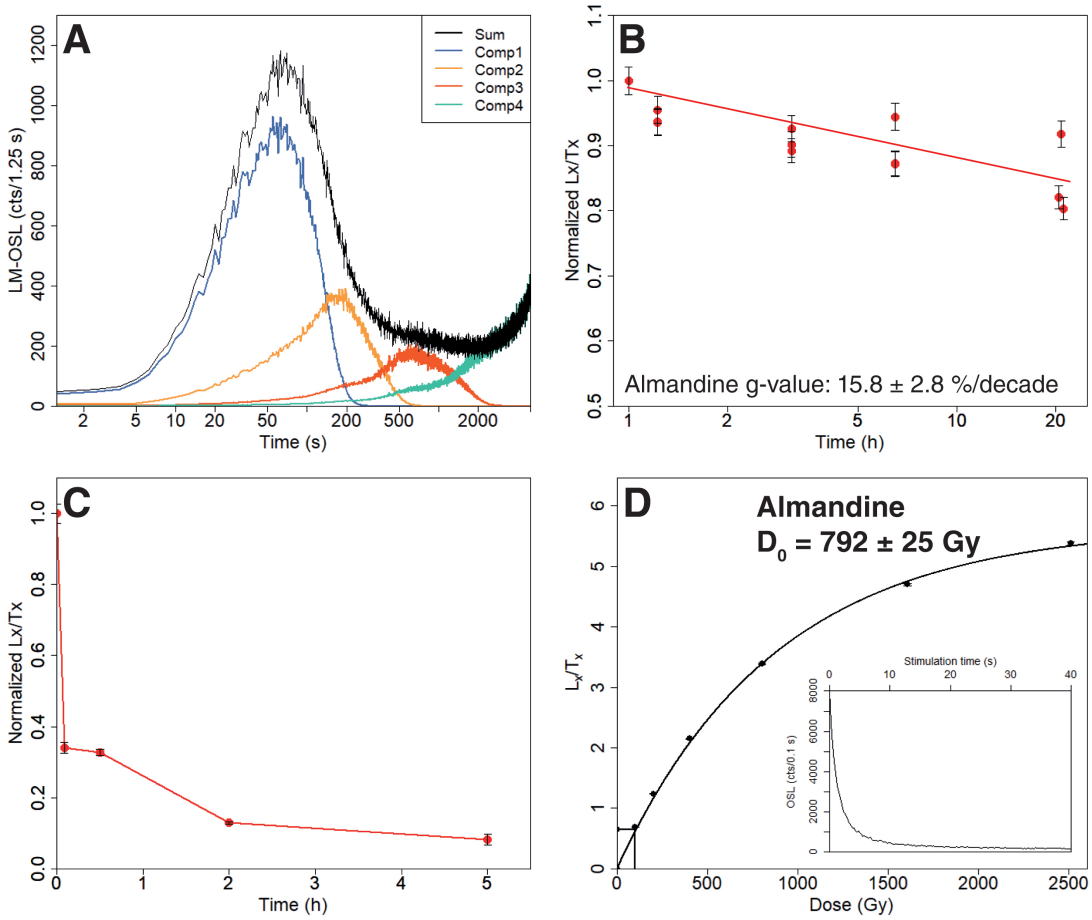

Figure 5. A) LM-OSL curve of almandine aliquot after a given dose of 200 Gy. Four OSL components resulted from deconvolution of the LM-OSL curve. B) Athermal decay of the OSL signal, with calculated g-value. C) Bleaching behavior represented by decay of the OSL signal in terms of light exposure time. D) Dose response curve showing the characteristic dose value (D_0)

and 325 °C TL peaks were determined from integration intervals of ± 20 °C centered at the corresponding TL peak (Fig. 7). A lower decrease rate is observed for the TL peak at 170 °C compared to the 90 °C TL peak (Fig. 7). As suggested by observation of the TL glow curves, the 325 °C TL peak shows stability under room temperature for the studied time interval (Fig. 7). All observed TL peaks decays with exposure to the solar simulator lamp (Fig. 6D).

IRSL and post-IR IRSL emission (blue-violet detection window) from kyanite aliquots show negligible intensities, impeding detection of signal over the observed background. The OSL decay curves of kyanite aliquots have decreasing intensities for higher preheat temperatures (Fig. 8). The LM-OSL emission has relatively low intensity, with a low peak at around 200 s. The low luminescence sensitivity of the kyanite impeded the identification of individual OSL components from the LM-OSL curves (Fig. 9A). Fading tests resulted in variable g-values from 10.4 to 33.6 %/decade with an average of 21.2 ± 11.6 %/decade (Fig. 9B). When exposed to a solar simulator lamp, the OSL signal (50 Gy) progressively decreases, confirming its bleachability (Fig. 9C). After 5 minutes of light exposure, the remaining OSL signal is around 50% of the initial signal. The remaining signal is 4% of the initial OSL signal after 5 hours of light exposure. The dose response curve is well described by a single-saturating exponential function (Fig. 9D), pointing to

Mineral	Calculated dose (Gy)	Calculated-to-given dose ratio	Recuperation (%)	Recycling ratio	D_0 (Gy)
Almandine	98.8 ± 4.4	0.98 ± 0.04	<0.1%	1.07 ± 0.04	791 ± 1
Kyanite	99.2 ± 9.3	0.99 ± 0.09	<0.1%	1.21 ± 0.16	1080 ± 139

Table 2. Summary of dose recovery test for a 100 Gy given dose. The results are the average of two aliquots. Measurement protocol described in Table 1.

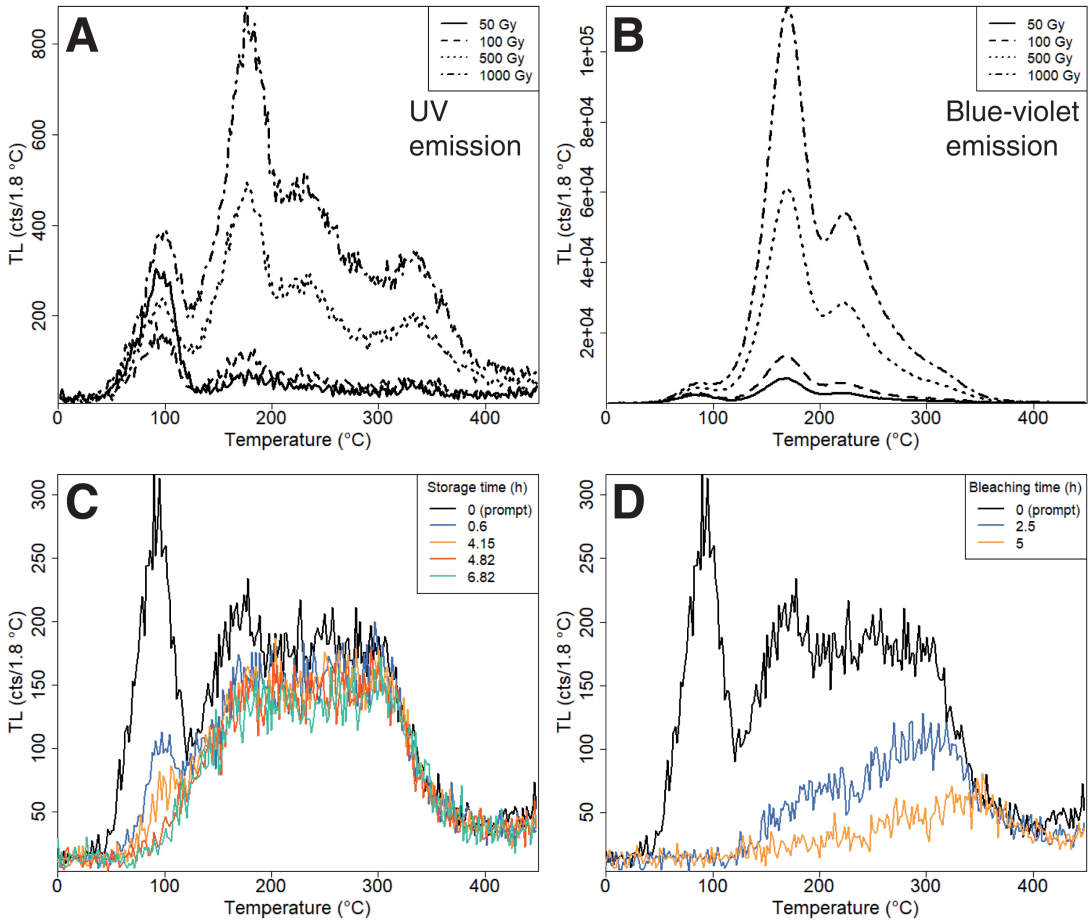

Figure 6. TL glow curves for the UV (A) and blue-violet (B) emissions from kyanite aliquots. C) TL glow curves obtained after different storage times at room temperature (given dose of 200 Gy). D) TL glow curves recorded after different bleaching times under a solar simulator lamp. Note that the same TL glow curve is used as reference for both stability and bleaching tests. Successive measurements were performed on the same aliquots.

an average D_0 value of 1080 Gy (n=2). Dose recovery tests present calculated-to-given dose ratio of 0.99 ± 0.09, with aliquots showing negligible recuperation (< 0.1%) and average recycling ratio of 1.21 ± 0.16 (Table 2).

4. Discussion

Almandine and kyanite are common detrital minerals in sandy sediments (Morton & Hallsworth, 1994, 1999) and they can potentially record equivalent doses used to determine sediment burial ages. Furthermore, these minerals are common in metamorphic rocks and their TL and OSL properties can be explored for surface exposure dating (Sohbati et al., 2012) and for low temperature thermochronology (King et al., 2016). Previous difficulties in isolating specific heavy minerals for luminescence dating (van Es et al., 2002) could be surpassed combining spatially resolved luminescence measurements (Kook et al., 2015) and mineral chemistry analysis using micro X-ray fluorescence methods (Thomsen et al., 2018). In this study, almandine shows a broad TL peak and IRSL and post-IR IRSL emissions, which are analogous to the luminescence characteristics of feldspar (Bøtter-Jensen et al., 1994; Blair et al., 2005). Kyanite has several discrete TL peaks, located approximately at 90, 170, 220 and 325 °C, as well as absence of IRSL emission, resembling the luminescence characteristics of quartz (Krbetschek et al., 1997). TL signals from almandine aliquots show instability as their TL intensities decreases with storage time at room temperature. Kyanite also presents unstable TL peaks, with exception of the TL peak at 325 °C. Both minerals present TL peaks sensitive to light. The TL glow curve from kyanite (Fig. 6) presents a behavior similar to quartz TL as it also displays a so-called "Rapidly Bleaching Peak" (RBP) at lower temperature (90 °C) and a "Slowly Bleaching Peak" (SBP) at higher temperature (325 °C) (Martini et al., 2009). The TL peak at 325 °C of kyanite decreases to around 30 – 40% of its initial intensity after 5 hours of light exposure, which is a rate similar to IRSL and post-IR IRSL signals from potassium feldspar (Buylaert et al., 2012). However, our experiments are unsuitable to discriminate the decay of

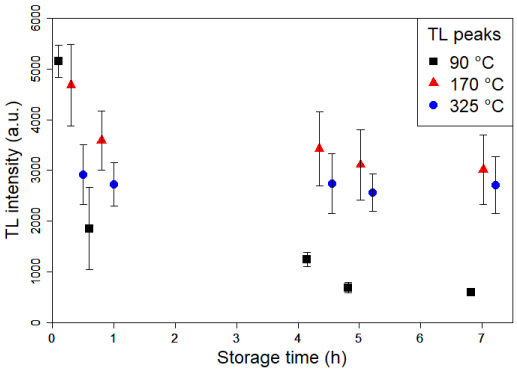

Figure 7. Intensity variation of TL peaks at 90, 170 and 325 °C (given dose of 200 Gy) from kyanite aliquots irradiated with 200 Gy and stored at room temperature for different times (storage time). Each TL intensity point is represented by the average of two aliquots. Data points are offset in the x axis to avoid points overlapping.

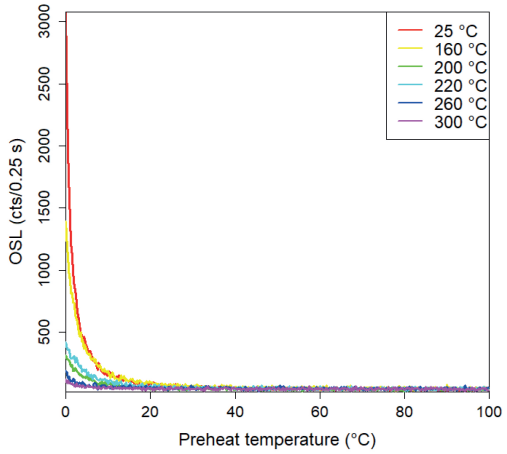

Figure 8. OSL decay curves of kyanite measured for different preheat temperatures (from 25 to 300 °C). Aliquots were irradiated with 100 Gy.

TL peaks from almandine and kyanite in terms of thermal or light bleaching effects. For example, such a loss of TL signal during storage at room temperature and light exposure experiments could be the result of thermal quenching, causing a reduced efficiency of the luminescence response to a given dose when the increase of temperature led to electrons recombining through non-radiative centers (Pagonis et al., 2010). Nonetheless, the difference in signal behavior between the TL curves obtained for the storage time (Fig. 2C, 6C) and bleaching experiments (Fig. 2D, 6D) cannot be explained entirely by thermal quenching since the main measurement parameters (i.e. heating rate, maximum temperature, given dose and dose rate) were the same during both experiments. Further experiments should be performed to clarify the process responsible for decay of TL signals observed in almandine and kyanite.

Both almandine and kyanite show an OSL emission in the UV band (blue stimulation). The OSL decay curve of almandine can comprise four OSL components. The OSL sensitivity of kyanite is extremely low (~ 0.5 cts Gy^{-1} mg^{-1} for the first second of light emission) which could hamper measuring doses below 100 Gy. The OSL signals from almandine and kyanite have relatively high fading rates, respectively with average g-values of 15.8 ± 2.8 %/decade and 21.2 ± 11.6 %/decade (Fig. 5B,9B), which are higher than g-values reported for the OSL signal from feldspar measured with blue stimulation and UV detection (g-value = 3.2 ± 0.2 %/decade, (Thomsen et al., 2008). The high variation in g-values found for kyanite points that fading rate should be estimated for individual aliquots for equivalent dose correction purposes. Also, due to such high g-values, signal loss during irradiation must be included in the estimation.

The OSL signals from almandine and kyanite decay to 10% of their initial value after 5 hours of exposure to a solar simulator lamp (Fig. 5C, 9C). This bleaching rate is also similar to that presented by feldspar IRSL and post-IR IRSL signals (Buylaert et al., 2012). In this case, residual signals for both minerals can promote significant dose overestimation and should be evaluated, especially for sediments experiencing fast deposition and short light exposure periods like in alluvial fans or braided rivers. The studied almandine and kyanite have dose response curves with D_0 reaching values higher than 700 Gy (Fig. 5D, 9D), which is beyond quartz OSL (Murray & Wintle, 2003) and similar to potassium feldspar post-IR IRSL (Buylaert et al., 2012). Dose recovery tests demonstrate the suitability of the studied minerals to recover a given dose (100 Gy) under laboratory conditions. However, the high fading rates are challenging for estimation of natural doses and potential extension of the age limit of luminescence dating.

Regarding dose rate assessment, uranium (^{238}U and ^{235}U), thorium (^{232}Th) and potassium (^{40}K) can occur as impurities in almandine and kyanite, contributing to significant internal dose rate. Almandine forms part of the garnet group that can be defined by the general formula $X_3Y_2(SiO_4)_3$, where the X position can be occupied by divalent cations of Ca^{2+}, Mg^{2+}, Fe^{2+} and Mn^{2+} and the Y position corresponds to trivalent cations as Al^{3+}, Fe^{3+} and Cr^{3+} (Deer et al., 2013). Almandine represents the ferric extreme ($Fe^{2+}{}_3Al_2(SiO_4)_3$) of the iron-magnesium solid solution series while pyrope is the magnesium extreme ($Mg_3Al_2(SiO_4)_3$). Kyanite is an aluminosilicate with general formula $Al_2(SiO_4)O$ and has andalusite and sillimanite as polymorphs (Deer et al., 2013). In the particular case of K, which promotes significant internal dose rate in potassium feldspar (Huntley & Baril, 1997), its relatively large atomic radius (Shannon, 1976) prevents substitution into the crystal lattice of both almandine and kyanite. However, chemical analysis on garnet crystals within metamorphic rocks (skarn) from Scotland (United Kingdom) indicates that the content of uranium could exceed 300 ppm (Smith et al., 2004) and in that case alpha particles are important contributors of the dose rate and most dose could be internal. This opens the possibility to explore chronometers

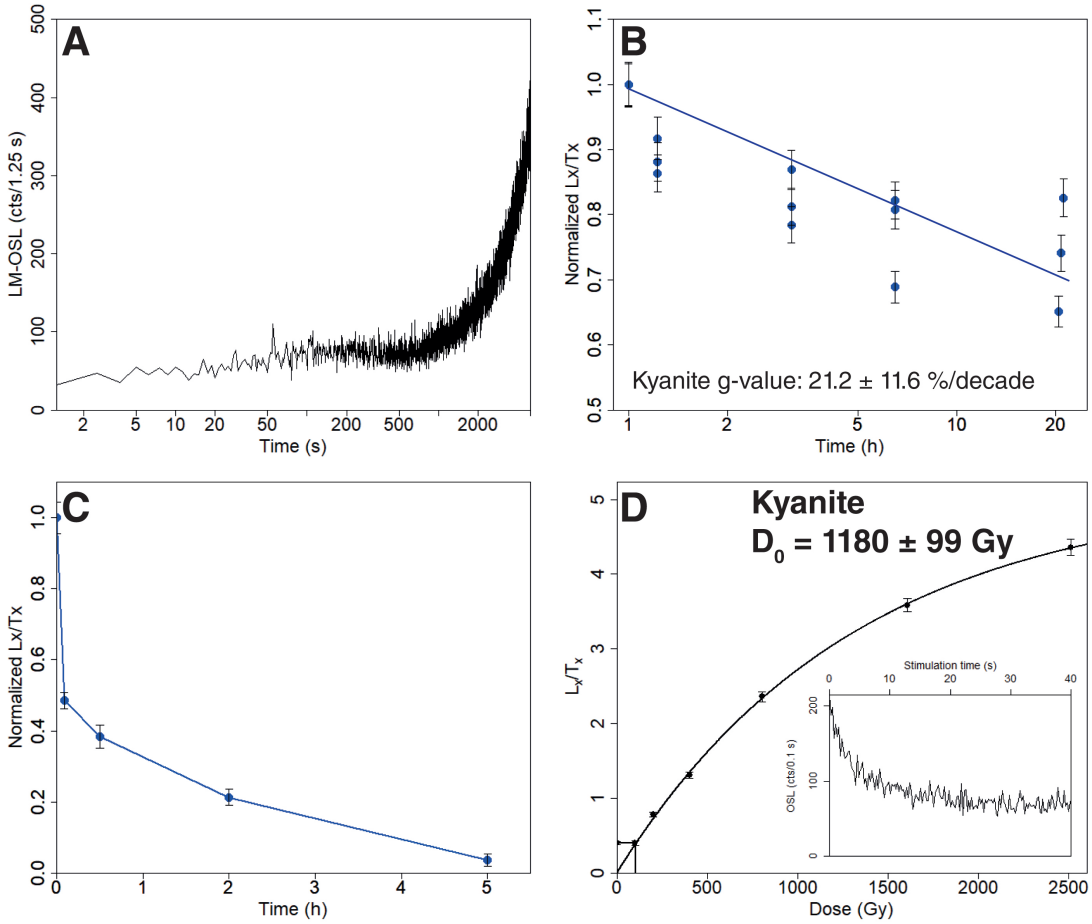

Figure 9. A) LM-OSL curve from a kyanite aliquot irradiated with 200 Gy. B) Athermal decay of the OSL signal, with calculated g-value. C) Bleaching behavior represented by decay of the OSL signal in terms of light exposure time. D) Dose response curve and calculated D_0 value.

based on natural regenerated signals like the method proposed for zircon (Smith, 1988; van Es et al., 2002). In such case, the assessment of radionuclides concentrations in minerals of the garnet group, like almandine, is needed for calculation of internal dose rate. In the studied almandine crystals, however, significant concentrations of U, Th or K were not detected using SEM/EDS (Fig. 1E).

5. Conclusions

IRSL and post-IR IRSL signals were observed only in almandine. Particularly, optical bleaching and stability of the 325 °C TL peak from kyanite deserve future investigations to evaluate its use for equivalent dose estimation. The OSL signals of almandine and kyanite are bleachable, with less than 10% of the initial signals remaining after 5 hours of light exposure. They present high saturation doses ($2D_0$ > 1500 Gy) that could extend the luminescence dating age limit beyond the mid Pleistocene, assuming dose rates of ~ 1 Gy/ka, typical of quartz-rich sands and of minerals hosting insignificant amounts of radionuclides. Dose recovery tests demonstrated that the studied heavy minerals can recover a given dose within unity under laboratory conditions. However, athermal stability and high fading rates of the studied OSL signal may entail a problem to obtain accurate equivalent doses estimates and ages. Future work should focus on searching for stable signals. Also, the investigation of the luminescence properties of other heavy minerals common in sediments (e.g. staurolite, sillimanite, titanite, apatite, epidote, rutile, tourmaline and zircon) is recommended for potential expansion of trapped-charged dating methods.

Acknowledgments

We are grateful to the Reviewer Prof. Ashok K. Singhvi for the insightful comments to improve the manuscript. We also thank the Editor Prof. Regina DeWitt for handling the manuscript. This research was conducted by funding provided by CONICYT (Chile) through the PhD Scholarship 21160616 provided to Ian Del Río. André O. Sawakuchi is supported by CNPq grant 304727/2017-2. We thank Dr. Flavio Machado de Souza Carvalho and Dr. Isaac Jamil Sayeg for their contributions with X-ray diffraction and SEM/EDS analysis.

References

Almeida, F. F. M., Brito Neves, B. B., and Carneiro, C. D. R. *The origin and evolution of the South American Platform* . Earth-Science Reviews, 50(1–2): 77–111, 2000. doi: 10.1016/S0012-8252(99)00072-0.

Auclair, M., Lamothe, M., and Huot, S. *Measurement of anomalous fading for feldspar IRSL using SAR*. Radiation Measurements, 37 (4–5): 487–492, 2003. doi: 10.1016/S1350-4487(03)00018-0.

Blair, M. W., Yukihara, E. G., and McKeever, S. W. S. *Experiences with single-aliquot OSL procedures using coarse-grain feldspars*. Radiation Measurements, 39(4): 361–374, 2005. doi: 10.1016/j.radmeas.2004.05.008.

Bøtter-Jensen, L., Duller, G. A. T., and Poolton, N. R. J. *Excitation and emission spectrometry of stimulated luminescence from quartz and feldspars*. Radiation Measurements, 23(2–3): 613–616, 1994. doi: 10.1016/1350-4487(94)90108-2.

Buylaert, J. P., Murray, A. S., Thomsen, K. J., and Jain, M. *Testing the potential of an elevated temperature IRSL signal from K-feldspar*. Radiation Measurements, 44(5–6): 560–565, 2009. doi: 10.1016/j.radmeas.2009.02.007.

Buylaert, J. P., Jain, M., Murray, A. S., Thomsen, K. J., Thiel, C., and Sohbati, R. *A robust feldspar luminescence dating method for Middle and Late Pleistocene sediments*. Boreas, 41: 435–451, 2012. doi: 10.1111/j.1502-3885.2012.00248.x.

Cano, N. F., Yauri, J. M., Watanabe, S., Mittani, J. C. R., and Blak, A. R. *Thermoluminescence of natural and synthetic diopside.* Journal of Luminescence, 128(7): 1185–1190, 2008. doi: 10.1016/j.jlumin.2007.11.090.

Cano, N. F., Blak, A. R., and Watanabe, S. *Electron paramagnetic resonance and the thermoluminescence emission mechanism of the 280 °C peak in natural andalusite crystal.* Journal of Luminescence, 131(7): 1545–1549, 2011. doi: 10.1016/j.jlumin.2011.02.014.

Deer, W. A., Howie, R. A., and Zussman, J. *An introduction to the rock-forming minerals*. Studies in archaeological science. Mineralogical Society of Great Britain and Ireland, 2013. doi: 10.1180/DHZ.

do Nascimento Jr, D., Sawakuchi, A., Guedes, C., Giannini, P., Grohmann, C., and Ferreira, M. *Provenance of sands from the confluence of the Amazon and Madeira rivers based on detrital heavy minerals and luminescence of quartz and feldspar*. Sedimentary Geology, 316: 1–12, 2015. doi: 10.1016/j.sedgeo.2014.11.002.

Duller, G. A. T. *The Analyst software package for luminescence data: overview and recent improvements* . Ancient TL, 33 (1): 35–42, 2015. URL http://ancienttl.org/ATL_33-1_2015/ATL_33-1_Duller_p35-42.pdf.

Guedes, C. C. F., Giannini, P. C. F., Nascimento Jr, D. R., Sawakuchi, A. O., Tanaka, A. P. B., and Rossi, M. G. *Controls of heavy minerals and grain size in a Holocene regressive barrier (Ilha Comprida, southeastern Brazil)*. Journal of South American Earth Sciences, 31(1): 110–123, 2011. doi: 10.1016/j.jsames.2010.07.007.

Hansen, V., Murray, A., Buylaert, J.-P., Yeo, E.-Y., and Thomsen, K. *A new irradiated quartz for beta source calibration*. Radiation Measurements, 81: 123–127, 2015. doi: 10.1016/j.radmeas.2015.02.017.

Huntley, D. J. and Baril, M. R. *The K content of the K-feldspars being measured in optical dating or in thermoluminescence dating*. Ancient TL, 15(1): 11–13, 1997. URL http://ancienttl.org/ATL_15-1_1997/ATL_15-1_Huntley_p11-13.pdf.

Huntley, D. J. and Lamothe, M. *Ubiquity of anomalous fading in K-feldspars, and the measurement and correction for it in optical dating*. Canadian Journal of Earth Sciences, 38(7): 1093–1106, 2001. doi: 10.1139/e01-013.

Jain, M., Murray, A., and Bøtter-Jensen, L. *Characterisation of blue-light stimulated luminescence components in different quartz samples: implications for dose measurement*. Radiation Measurements, 37(4-5): 441–449, 2003. doi: 10.1016/j.radmeas.2015.02.017.

King, G. E., Guralnik, B., Valla, P. G., and Herman, F. *Trapped-charge thermochronometry and thermometry: A status review*. Chemical Geology, 446(23): 3–17, 2016. doi: 10.1016/j.chemgeo.2016.08.023.

Kook, M., Lapp, T., Murray, A. S., Thomsen, K. J., and Jain, M. *A luminescence imaging system for the routine measurement of single-grain OSL dose distributions*. Radiation Measurements, 81(4-5): 171–177, 2015. doi: 10.1016/j.radmeas.2015.02.010.

Krbetschek, M. R., Götze, J., Dietrich, A., and Trautmann, T. *Spectral information from minerals relevant for luminescence dating*. Radiation Measurements, 27(506): 695–748, 1997. doi: 10.1016/S1350-4487(97)00223-0.

Kreutzer, S., Schmidt, C., Fuchs, M. C., Dietze, M., Fischer, M., and Fuchs, M. *Introducing an R package for luminescence dating analysis*. Ancient TL, 30(1): 1–8, 2012. URL http://ancienttl.org/ATL_30-1_2012/ATL_30-1_Kreutzer_p1-8.pdf.

Martini, M., Fasoli, M., and Galli, A. *Quartz OSL emission spectra and the role of [AlO4]° recombination centres*. Radiation Measurements, 44(5–6): 458–461, 2009. doi: 10.1016/j.radmeas.2009.04.001.

Morton, A. and Hallsworth, C. *Identifying provenance-specific features of detrital heavy mineral assemblages in sandstones*. Sedimentary Geology, 90(3–4): 241–265, 1994. doi: 10.1016/0037-0738(94)90041-8.

Morton, A. and Hallsworth, C. *Processes controlling the composition of heavy mineral assemblages in sandstones*. Sedimentary Geology, 124(1–4): 3–29, 1999. doi: 10.1016/S0037-0738(98)00118-3.

Murray, A. and Wintle, A. *The single aliquot regenerative dose protocol: potential for improvements in reliability*. Radiation Measurements, 37(4-5): 377–381, 2003. doi: 10.1016/S1350-4487(03)00053-2.

Nathan, R., Thomas, P., Jain, M., Murray, A., and Rhodes, E. *Environmental dose rate heterogeneity of beta radiation and its implications for luminescence dating: Monte Carlo modelling and experimental validation*. Radiation Measurements, 37(4-5): 305–313, 2003. doi: 10.1016/S1350-4487(03)00008-8.

Pagonis, V., Ankjaergaard, C., Murray, A., Jain, M., Chen, R., Lawless, J., and Greilich, S. *Modelling the thermal quenching mechanism in quartz based on time-resolved optically stimulated luminescence*. Journal of Luminescence, 130(5): 902–909, 2010. doi: 10.1016/j.jlumin.2009.12.032.

Rimington, N., Cramp, A., and Morton, A. *Amazon Fan sands: implications for provenance*. Marine and Petroleum Geolog, 17 (2): 267–284, 2000. doi: 10.1016/S0264-8172(98)00080-4.

Shannon, R. *Revised effective ionic radii and systematic studies of interatomic distances in halides and chalcogenides*. Acta Crystallographica, 32(5): 751–767, 1976. doi: 10.1107/S0567739476001551.

Smith, B. *Zircon from sediments: A combined OSL and TL autoregenerative dating technique*. Quaternary Science Reviews, 7 (3–4): 401–406, 1988. doi: 10.1016/0277-3791(88)90036-4.

Smith, M., Henderson, P., Jeffries, T., Long, J., and Williams, C. *The Rare Earth Elements and Uranium in Garnets from the Beinn an Dubhaich Aureole, Skye, Scotland, UK: Constraints on Processes in a Dynamic Hydrothermal System*. Journal of Petrology, 45(3): 457–484, 2004. doi: 10.1093/petrology/egg087.

Sohbati, R., Murray, A., Chapot, M., and Jain, M. *Optically stimulated luminescence (OSL) as a chronometer for surface exposure dating*. Journal of Geophysical Research, 117: B09202, 2012. doi: 10.1029/2012JB009383.

Souza, S., Selvin, P., and Watanabe, S. *Thermally stimulated luminescence, optical absorption and EPR studies on kyanite crystals*. Journal of Luminescence, 130(102-103): 575–580, 2003. doi: 10.1016/S0022-2313(02)00622-1.

Thomsen, K. J., Kook, M., Murray, A. S., and Jain, M. *Resolving luminescence in spatial and compositional domains.* Radiation Measurements, 120: 260–266, 2018. doi: 10.1016/j.radmeas.2008.06.002.

Thomsen, K., Murray, A., Jain, M., and Bøtter-Jensen, L. *Laboratory fading rates of various luminescence signals from feldspar-rich sediment extracts*. Radiation Measurements, 43(9–10): 1474–1486, 2008. doi: 10.1016/j.meas.2018.06.002.

van Es, H., Vainshtein, D., Rozendaal, A., Donoghue, J., Meijer, R., and den Hartog, H. *Thermoluminescence of ZrSiO4 (zircon): A new dating method?* Nuclear Instruments and Methods in Physics Research Section B: Beam Interactions with Materials and Atoms, 191(1-4): 649–652, 2002. doi: 10.1016/S0168-583X(02)00627-4.

Watanabe, S., Cano, N., Carmo, L., Barbosa, R., and Chubaci, J. *High- and very-high-dose dosimetry using silicate minerals*. Radiation Measurements, 72: 66–69, 2015. doi: 10.1016/j.radmeas.2014.11.004.

Reviewer

Ashok Singhvi